Journal of Alloys and Compounds 408–412 (2006) 628–631

Journal of ALLOYS AND COMPOUNDS

www.elsevier.com/locate/jallcom

Structural change in Sm- and Nd-doped ceria under a low oxygen partial pressure

Soichiro Sameshima, Yoshihiro Hirata*, Yuka Ehira

Department of Advanced Nanostructured Materials Science and Technology, Kagoshima University,
1-21-40 Korimoto, Kagoshima 890-0065, Japan

Received 30 July 2004; received in revised form 24 November 2004; accepted 15 December 2004

Abstract

The electromotive force (EMF) of Sm-doped ceria (SDC) and Nd-doped ceria (NDC) with Pt electrodes was measured using air and a H_2/H_2O gas or an Ar/O_2 gas in the oxygen partial pressure range from 10^0 to 10^{-25} Pa at 773–1173 K. The transport numbers of oxide ions (t_i) of SDC and NDC at 1073 K were 0.72–0.81 in the H_2/H_2O gas and 0.25–0.26 in the Ar/O_2 gas at 10^{-12} to 10^{-15} Pa of oxygen partial pressure, respectively. The heating of SDC and NDC in a H_2/H_2O gas of 10^{-15} Pa of oxygen partial pressure at 973 K for 1 h released 26–31% of the lattice oxygen atoms. The X-ray diffraction (XRD) patterns for the reduced SDC and NDC corresponded to those of cubic CeO_2 solid solution. However, the X-ray photo-emission spectra (XPS) of the reduced SDC and NDC showed the formation of Ce^{3+} ions.

Keywords: Energy storage materials; Chemical synthesis; X-ray diffraction; Electrochemical reactions; Ionic conduction

1. Introduction

The solid oxide fuel cell (SOFC) has received a considerable attention as an environment-friendly electric power generation device because of its high energy conversion efficiency and the clean product (H_2O) [1]. Rare earth-doped ceria (RDC) has a higher oxide ion conductivity than yttria-stabilized zirconia (YSZ) electrolyte [2–11]. The high ionic conductivity leads to the decrease of operation temperature of SOFC, which increases the lifetime and expands the choice of the constituent materials used for the electrodes and interconnector of SOFC. The problem pointed out on RDC is the increased electronic conduction at a low oxygen partial pressure, which is accompanied by the reduction of Ce^{4+} to Ce^{3+} [6,7,9,12,13]. The oxygen partial pressure at which the ionic conductivity is equal to the electronic conductivity, has been reported as follows at 1073 K: 10^{-10} Pa for $Ce_{0.8}Sm_{0.2}O_{1.9}$ (SDC) [6], 10^{-8} Pa for $Ce_{0.8}Gd_{0.2}O_{1.9}$ (GDC) [6], and 10^{-12} Pa for $Ce_{0.8}Gd_{0.2}O_{1.9}$ [7]. This paper reports on the structural change in Sm-doped ceria (SDC) and Nd-doped ceria (NDC) under a low oxygen partial pressure. The electromotive force (EMF) of both the electrolytes using air and a H_2/H_2O gas or an Ar/O_2 gas in the oxygen partial pressure range from 10^0 to 10^{-25} Pa was measured at 773–1173 K. The structures of SDC and NDC heated at a low oxygen partial pressure were also evaluated by X-ray diffraction (XRD), scanning electron microscope (SEM) and X-ray photo-emission spectra (XPS).

2. Experimental procedure

The RDC powder with a composition $Ce_{0.8}R_{0.2}O_{1.9}$ (R = Sm, Nd) was produced by heating the oxalate precursor $(Ce_{0.8}R_{0.2})_2(C_2O_4)_3$ at 873 K. The detail of the powder preparation method is reported in our previous papers [14,15]. An aqueous suspension of 35 vol.% SDC or NDC powder was prepared at pH 8 and polyacrylic ammonium (dispersant) of 0.25 mg/m^2 was added to the suspension. The suspension was consolidated to a disk of 22 mm diameter and 2 mm thickness by filtration through a gypsum mold. The consolidated disk

---

[*] Corresponding author. Tel.: +81 99 285 8325; fax: +81 99 257 4742.
E-mail address: hirata@apc.kagoshima-u.ac.jp (Y. Hirata).

0925-8388/$ – see front matter © 2005 Elsevier B.V. All rights reserved.
doi:10.1016/j.jallcom.2004.12.072

was pressed isostatically under a pressure of 294 MPa and sintered at 1773 K for 4 h in air (SPM 6512 electric furnace, Marusho Electro-Heat Co. Ltd., Japan). The electromotive force of SDC and NDC with Pt electrodes was measured using air and a H_2/H_2O gas or an Ar/O_2 gas at 773–1173 K. The oxygen partial pressure in an Ar gas was controlled in the range from 10^0 to 10^{-15} Pa by passing the Ar gas into an oxygen pump using YSZ (KOC-200B, Kaken Inc. Ibaraki, Japan). This pump separates electrochemically O_2 molecules from Ar gas. The oxygen partial pressure in the H_2/H_2O gas or Ar/O_2 gas was monitored with a YSZ oxygen sensor (KOA-200, Kaken Inc., Ibaraki, Japan). The sintered SDC and NDC were heated at 973 K for 1 h in a H_2/H_2O gas under an oxygen partial pressure of 10^{-15} Pa to evaluate their microstructures (SM-300, Topcon, Co., Tokyo, Japan). XPS spectra were recorded on an ESCA machine (ESCA 1000, Shimadzu Co., Kyoto, Japan). The base pressure during the analysis was 1.3×10^{-3} Pa. The sintered SDC and NDC were sputtered by Ar ions for 40 min. Calibration of the spectra was made using the lowest kinetic energy peak (binding energy 917.0 eV) of the Ce (3d) spectrum [16].

3. Experimental results and discussion

3.1. Transport number of oxide ion

Fig. 1 shows the transport number (t_i) of oxide ion calculated from the electromotive force (EMF) for SDC and NDC in the H_2/H_2O gas at 773–1173 K. The t_i values of SDC and NDC were in the range from 0.75 to 0.81 at 1073 K under an oxygen partial pressure of 10^{-12} to 10^{-15} Pa. No significant difference of t_i values between SDC and NDC was measured. The previously reported oxygen partial pressure for $t_i = 0.5$ at 1073 K is 10^{-10} Pa for SDC [6], 10^{-8} Pa for GDC [6] and 10^{-12} Pa for GDC [7]. Compared with these t_i values, the present samples showed the significantly high t_i values. This result is favorable to apply RDC for the solid electrolyte of SOFC. The solid lines in Fig. 1 correspond to the t_i values for SDC calculated from the electronic conductivity of SDC measured by the authors' group through the Hebb–Wagner method and the oxide ion conductivity measured in air [17]. Both the t_i values by the EMF method and Hebb–Wagner method provided the similar t_i values at 973 and 1073 K. The discrepancy of the t_i values at 773 and 873 K between the two methods is under investigation.

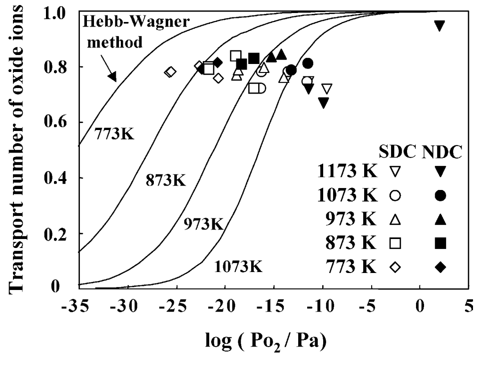

Fig. 1. Transport number of oxide ion (t_i) measured by electromotive force method for SDC and NDC in a H_2/H_2O gas at 773–1173 K. The solid lines correspond to the t_i values for SDC determined from the electronic conductivity by the Hebb–Wagner method and the oxide ion conductivity measured in air.

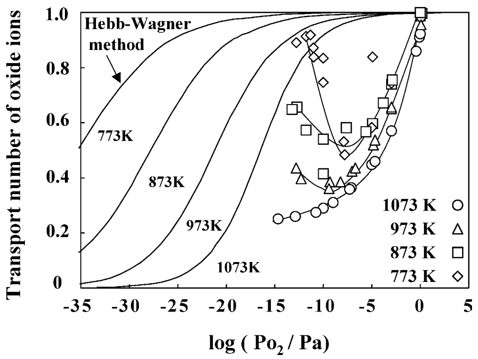

Fig. 2. Transport number of oxide ion measured by electromotive force for SDC in an Ar/O_2 gas at 773–1173 K. The solid lines correspond to the t_i values for SDC determined from the electronic conductivity by the Hebb–Wagner method and the oxide ion conductivity measured in air.

Fig. 2 shows the t_i values of oxide ion for the SDC in the Ar/O_2 gas at 773–1073 K. The t_i values decreased rapidly with decreasing oxygen partial pressure and showed a minimum at the oxygen partial pressure range of 10^{-7} to 10^{-10} Pa. The recovery of t_i values at the low oxygen partial pressures may be associated with the enhanced oxide ion diffusion through the increased concentration of oxygen vacancy, as explained below. In a lower oxygen partial pressure, the possible interaction between electron and Ce site or O site in SDC or NDC was expressed by Eqs. (1)–(4).

$$O_O^{\times} \leftrightarrows \frac{1}{2}O_2 + V_O^{\bullet\bullet} + 2e' \qquad (1)$$

$$Ce_{Ce}^{\times} + O_O^{\times} \rightleftarrows Ce'_{Ce} + V_O^{\bullet\bullet} + e' + \frac{1}{2}O_2 \qquad (2)$$

$$2Ce_{Ce}^{\times} + O_O^{\times} \leftrightarrows 2Ce'_{Ce} + V_O^{\bullet\bullet} + \frac{1}{2}O_2 \qquad (3)$$

$$Ce_{Ce}^{\times} + 2O_O^{\times} \leftrightarrows Ce'_{Ce} + 2V_O^{\bullet\bullet} + 3e' + O_2 \qquad (4)$$

For instance, the neutrality condition of electric charge for Eq. (2) is expressed by $2[V_O^{\bullet\bullet}] = [R'_{Ce}] + [Ce'_{Ce}] + [e']$. The equilibrium constant K for Eq. (2) is also given by $K = [Ce'_{Ce}][V_O^{\bullet\bullet}][e']Po_2^{1/2}/[Ce_{Ce}^{\times}][O_O^{\times}]$. In the condition $2[V_O^{\bullet\bullet}] = [Ce'_{Ce}]$, the above relationship gives the following concentration of the hopping electron: $[e'] = (2K)^{1/2}([Ce_{Ce}^{\times}][O_O^{\times}]/[Ce'_{Ce}])^{1/2}Po_2^{-1/4}$. All the cases were analyzed and the oxygen partial pressure dependence of the electron concentration was summarized in our recent paper [13]. The formed electron or hopping of electron in Ce'_{Ce} increases the electronic conduction. In addition, the formation of oxygen vacancy in Eqs. (1)–(4) may affect the

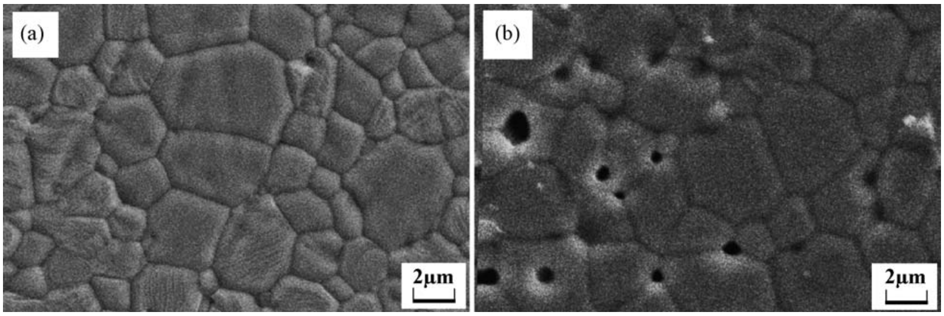

Fig. 3. Microstructure of (a) as-sintered SDC and (b) reduced SDC. The sintered SDC was heated at 973 K for 1 h in a H_2/H_2O gas under an oxygen partial pressure of at 10^{-15} Pa.

diffusion of oxide ion. A crucial factor affecting the difference of the results in Figs. 1 and 2 may be the presence of H_2O. In the presence of H_2O, H_2O may react with the oxygen vacancy in SDC or NDC as expressed by Eq. (5).

$$V_O^{\bullet\bullet} + H_2O \leftrightarrows O_O^{\times} + H_2 + 2h^{\bullet} \tag{5}$$

The produced hole reacts with the electron expressed in Eqs. (1)–(4). This reaction reduces the concentration of free or hopping electron in SDC or NDC and increases the t_i value.

3.2. Microstructure and X-ray diffraction analysis

Fig. 3(a) and (b) show the microstructures of SDC before and after the heating at 973 K for 1 h in a H_2/H_2O gas at 10^{-15} Pa of oxygen partial pressure, respectively. The SDC before the heating consisted of dense microstructure and average grain size was 2.2 μm. After the heating, many pores of submicrometer size were observed. These pores were mainly located at grain boundaries and produced by the release of oxygen gas (Eqs. (1)–(4)) from O sites in SDC. A similar structural change was also observed in NDC. The relative density of SDC and NDC decreased as follows by heating: 97.1% → 93.0% for SDC and 97.7% → 92.5% for NDC. This change of density indicates that lattice oxygen atoms of 26.3–31.1% were released by the heating at 973 K under the reduced atmosphere. However, the X-ray diffraction patterns of SDC and NDC after hearting were identified as those of a cubic fluorite structure for CeO_2 solid solution.

3.3. X-ray photo-emission spectra

Fig. 4(A) shows XPS spectra in Ce 3d region for as-sintered (a, b) and reduced (c, d) SDC and NDC. The large peaks of u''' (917 eV), v''' (899 eV), u (901 eV) and v (883 eV), and small peaks of u'' (908 eV) and v'' (889 eV) appeared in the as-sintered SDC (a) and NDC (b). These six peaks were characterized by 3d electron of Ce^{4+} [18]. On the other hand, the reduced SDC (c) and the reduced NDC (d), which were heated at 973 K at 10^{-15} Pa of oxygen partial pressure, provided four peaks of u' (905 eV), v' (887 eV), u_0 (900 eV) and v_0 (882 eV), which corresponded to Ce^{3+} species [18]. Fig. 4(B) shows XPS spectra in O 1s region for the four samples. O 1s spectrum observed at 529.5 eV in (a) shifted to the higher binding energy at 530.1 eV in (c) by reducing the SDC. Leachir et al. reported that the O 1s peak tended to shift towards the higher binding energy upon reduction by hydrogen [19]. However, no shift of O 1s peak was observed for NDC after the reduction.

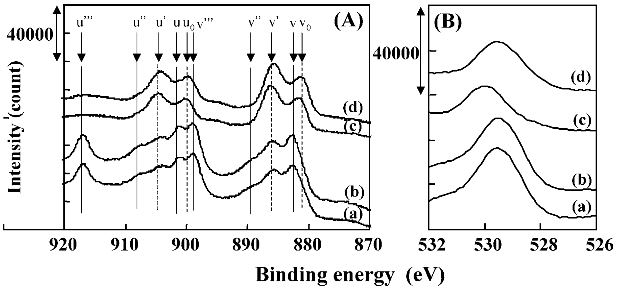

Fig. 4. XPS Ce 3d emission spectra (A) and O 1s emission spectra (B) of (a) as-sintered SDC, (b) as-sintered NDC, (c) reduced SDC and (d) reduced NDC after sputtering by Ar^+ for 40 min.

4. Conclusions

1. The transport number of oxide ions for SDC and NDC were 0.75–0.81 at 1073 K at an oxygen partial pressure of 10^{-12} to 10^{-15} Pa of a H_2/H_2O gas. As compared with the result in the H_2/H_2O gas, the transport number of oxide ions in an Ar/O_2 gas decreased greatly.
2. Lattice oxygen atoms of 26.3–31.1% in SDC and NDC were released by heating at 973 K under an oxygen partial pressure of 10^{-15} Pa and many pores of submicrometer-size were produced in SDC and NDC.
3. Although the reduced SDC and NDC showed X-ray diffraction patterns of a cubic fluorite structure, the presence of Ce^{3+} ion was confirmed by XPS.

Acknowledgements

The authors would like to thank Mr. Y. Ohzono (Center for Instrumental Analysis, Kagoshima University) for the measurement of XPS.

References

[1] N.Q. Minh, J. Am. Ceram. Soc. 76 (1993) 563–588.
[2] T.H. Etsell, S.N. Flengas, Chem. Rev. 70 (1970) 339–376.
[3] T. Kudo, H. Obayashi, J. Electrochem. Soc. 122 (1975) 142–147.
[4] H.L. Tuller, A.S. Nowick, J. Electrochem. Soc. 122 (1975) 255–259.
[5] R.T. Dirstine, R.N. Blumenthal, T.F. Kuech, J. Electrochem. Soc. 126 (1979) 264–269.
[6] H. Yahiro, K. Eguchi, H. Arai, Solid State Ionics 36 (1989) 71–75.
[7] B.C.H. Steel, K. Zheg, R.A. Rudkin, N. Kiratzis, M. Chrisitie, in: M. Dokiya, O. Yamamoto, H. Tagawa, S.C. Singhal (Eds.), Proceedings of the 4th International Symposium on Solid Oxide Fuel cells (SOFC IV), The Electrochem.Soc. Inc., New Jersy, 1995, pp. 1028–1038.
[8] H. Inaba, H. Tagawa, Solid State Ionics 83 (1996) 1–16.
[9] K. Eguchi, J. Alloys Compd. 250 (1997) 486–491.
[10] Y. Hirata, H. Ono, K. Higashi, K. Sonoda, S. Sameshima, Y. Ikuma, Ceram. Trans. 92 (1999) 137–148.
[11] S. Sameshima, H. Ono, K. Higashi, K. Sonoda, Y. Hirata, Y. Ikuma, J. Ceram. Soc. Jpn. 108 (2000) 1058–1064.
[12] T. Mori, T. Ikegami, H. Yamamura, J. Electrochem. Soc. 146 (1999) 4380–4385.
[13] T. Shimonosono, Y. Hirata, Y. Ehira, S. Sameshima, T. Horita, H. Yokokawa, Solid State Ionics 174 (2004) 27–33.
[14] K. Higashi, K. Sonoda, H. Ono, S. Sameshima, Y. Hirata, Key Eng. Mater. 159–160 (1999) 25–30.
[15] K. Higashi, K. Sonoda, H. Ono, S. Sameshima, Y. Hirata, J. Mater. Res. 14 (1999) 957–967.
[16] J.P. Holgado, R. Alvarez, G. Munuera, Appl. Surf. Sci. 161 (2000) 301–315.
[17] T. Shimonosono, Y. Hirata, Y. Ehira, S. Sameshima, T. Horita, J. Ceram. Soc. Jpn. Suppl. 112 (2004) S616–S621.
[18] P. Burroughs, A. Hammett, A.F. Orchard, G.J. Thornton, J. Chem. Soc. Dalton Trans. 17 (1976) 1686–1698.
[19] A. Leachir, V. Perrichon, A. Badri, J. Lamotte, E. Catherine, J.C. Lavalley, J. El Fallah, L. Hilaire, F. LeNormand, E. Quéméré, G.N. Sauvion, O. Touret, J. Chem. Soc. Farady Trans. 97 (1991) 1601–1609.